# Fluorescent Visualization of Bond Breaking in Polymer Glasses

Macromolecules

pubs.acs.org/Macromolecules

Article

# Fluorescent Visualization of Bond Breaking in Polymer Glasses

Annelore Aerts, Stan F.S.P. Looijmans, Lambèrt C.A. van Breemen, Rint P. Sijbesma,* and Johan P.A. Heuts*

Cite This: *Macromolecules* 2023, 56, 4267−4277

Read Online

ACCESS | Metrics & More | Article Recommendations | Supporting Information

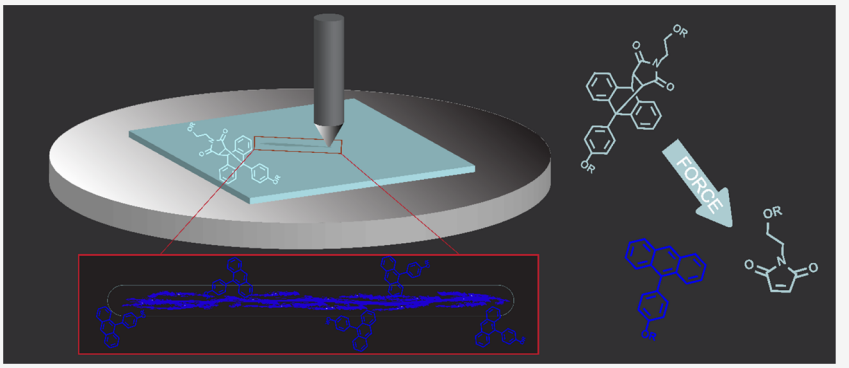


**ABSTRACT:** Mechanofluorescent polymer probes were used to visualize stresses and bond scission in polystyrene and polycarbonate. Sonication of polystyrene probes with a molar mass of $1.1 \times 10^5$ g·mol$^{-1}$ in solution resulted in 30% activation after 1 h, while shorter probes showed lower activation percentages. Single-asperity sliding friction tests were performed on mechanophore-containing polystyrene and polycarbonate films. Polystyrene showed clearly visible crack formation with a correlated pattern in the friction force, penetration depth, and fluorescent activation of the mechanophore. Significant mechanophore activation in polystyrene was observed for an applied normal load of 100 mN, whereas in polycarbonate, activation only occurred at a normal load higher than 400 mN. The different degrees of activation correlate well with the toughness of polycarbonate compared to polystyrene.



## INTRODUCTION

Glassy polymers are extensively used in a wide range of applications, in which the severity of the demands can result in premature failure of the materials.[1−3] Failure often starts with a small imperfection, which initiates the formation of a small crack that grows to ultimately make the material fail, limiting the useful lifetime and performance of glassy polymers.[3−5] Hence, it is of great importance to get a better understanding of the structure−property relationships of polymers and their failure mechanisms in order to be able to predict the long-term mechanical behavior of a material and to ensure its reliability for safety reasons.[6,7] Numerous studies have shown that force-responsive molecular units, generally known as mechanophores, are useful instruments to study the behavior of polymers under stress.[8−13] Mechanophores change their optical properties when a stress is applied; the most common detection methods are mechanochromism,[14] mechanoluminescence,[15] and mechanofluorescence.[16,17] Mechanochromism has been studied extensively, with the use of spiropyrans as the most defined and well-studied example. Mechanoluminescence was introduced by our group in 2012 with the chemiluminescent response of 1,2-dioxetane upon exposure to stress.[10,15] For a study of bond scission in glassy polymers under stress, both absorption and chemiluminescence-based techniques have limitations, such as low sensitivity in absorption and a limited luminescent lifetime.[18] In the current study, we therefore use a sensitive and time-independent stress visualization method based on the well-known mechanofluorescent anthracene−maleimide Diels−Alder adduct.[16,19] Most mechanophore studies on non-cross-linked systems were performed on elastomers, in which stresses can be visualized prior to failure of the material because the forces are mostly transduced along the backbone. For many glassy materials, however, covalent bond scission is not expected to occur frequently over a detectable area before failure, and hence, stress detection in glassy polymers remains a challenge. Activation of spiropyran in PMMA was studied by Moore and co-workers, who showed that compression of spherical beads leads to activation just beyond the yield point [ref 14]. Mechanophore activation in other glassy polymers has been studied infrequently and has mostly been achieved under specialized force conditions, such

**Received:** December 1, 2022
**Revised:** May 10, 2023
**Published:** May 26, 2023

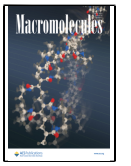

Scheme 1. Chemical Structures of the Mechanophore (AM) and the Mechanophore-Containing Polymers PS1−PS5 and PC

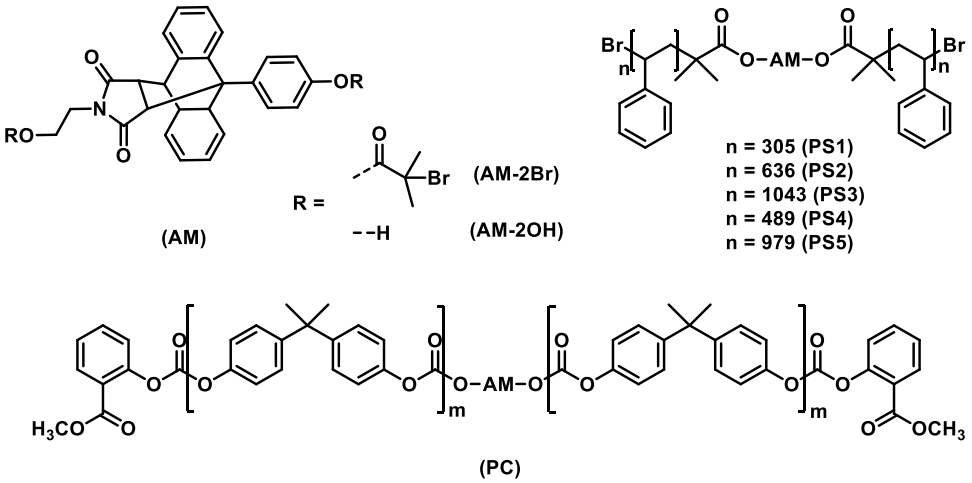


as torsional shearing, shockwaves, and by tensile forces on an adapted polymer system at elevated temperatures or in the presence of a plasticizer.[20−22] Mechanical activation of diarylacetonitrile radical-forming mechanophores by grinding of polystyrene has been reported by Otsuka and co-workers.[23] Recently, Vidavsky[24] and co-workers were the first to report mechanochemical activation under tensile stresses in polycarbonate without the need of elevated temperatures or additives. Mechanophore activation in a sliding friction test on an epoxy thermoset under transient loading conditions and with extreme stress localization has been published by Davis et al.[25]

Polystyrene (PS) and polycarbonate (PC) are commercially important glassy polymers with remarkably different mechanical properties. Polystyrene is known to undergo brittle failure, whereas polycarbonate is a tougher material.[26] While the origin of this difference is reasonably well understood at the mesoscopic level, correlation of macroscopic failure with the extent of bond scission at the molecular scale has not been investigated in detail but is of great importance for a full understanding of the mechanical behavior of these polymers.

Here, we present the fluorescent visualization of bond scission in polystyrene and polycarbonate glasses. A π-extended anthracene−maleimide Diels−Alder adduct (Scheme 1) was synthesized, characterized as a mechanophore, and incorporated into polystyrene and polycarbonate via a single-electron transfer-living radical polymerization (SET-LRP) and a solution trans carbonation, respectively. Mechanochemical activation was tested in solution and in the solid state.

## RESULTS

**Synthesis of Polymer Mechanophores.** Anthracene−maleimide Diels−Alder cycloadduct AM (Scheme 1) was synthesized and used as a mechanophore in glassy polymers. AM was obtained in a multistep synthesis (see the Supporting Information (SI) and the Experimental Details Section for details) and incorporated into polystyrene (PS1−PS5, Scheme 1) or polycarbonate (PC, Scheme 1). For the polystyrene-based probe, a bifunctional ATRP initiator (AM-2Br) was synthesized, and polystyrene was grown simultaneously on both sides of the AM mechanophore via a single-electron transfer-living radical polymerization (SET-LRP). For the polystyrene-based probe, a bifunctional ATRP initiator (AM-2Br) was synthesized, and polystyrene was grown simultaneously on both sides of the AM mechanophore via a single-electron transfer-living radical polymerization (SET-LRP). Since we do not expect a significant difference in the initiation rate between the two initiator groups and we do not have indications of significant termination (maybe with the exception of PS4, see Figure S1), this approach results in polystyrene chains with a centrally located mechanophore. The adjacent polymer chains play an important role in the propagation of the generated forces on the polymer toward the mechanophore.[12] Polystyrene polymers of five different molar masses (PS1−PS5, Table 1) were synthesized (for molar mass distributions, see Figure S1). Additionally, bisphenol-A polycarbonate was synthesized via solution polymerization.[27,28] A prepolymer of polycarbonate (PC-prepol) was synthesized and coupled with AM-2OH to obtain a mechanophore-functionalized polycarbonate (see the SI for details). In this polymer, the mechanophore is not necessarily situated in the center of the chain, and in some cases, more than one mechanophore is likely built into the polymer. Diffusion-ordered spectroscopy (DOSY)-NMR (Figure S2) was used to confirm the incorporation of the mechanophore. It clearly shows the same diffusion coefficient for the polymer peaks and the mechanophore peaks. For both polystyrene and polycarbonate, the total length of the polymers significantly exceeds the molar masses between entanglements, which are $M_{e,PS} \approx 15 \times 10^3$ g·mol$^{-1}$ and $M_{e,PC} \approx 2.5 \times 10^3$ g·mol$^{-1}$.[29] This is

Table 1. Number-Average Molar Masses and Dispersities of the Polymers Used in this Study

| polymer | $M_n$[a] [g·mol$^{-1}$] | $Đ$[b] |
|---|---|---|
| PS1 | $32 \times 10^3$ | 1.2 |
| PS2 | $66 \times 10^3$ | 1.5 |
| PS3[c] | $109 \times 10^3$ | 1.2 |
| PS4 | $51 \times 10^3$ | 1.4 |
| PS5[cc] | $102 \times 10^3$ | 1.3 |
| PC-prepol | $10 \times 10^3$ | 2.1 |
| PC | $31 \times 10^3$ | 1.8 |
| PSS | $107 \times 10^3$ | 1.8 |
| PSL | $560 \times 10^3$ | 1.9 |

[a]Number-average molar mass as determined by SEC. [b]$Đ \equiv M_w/M_n$ as determined by SEC. [c]PS3 and PS5 can be considered to be two different batches of the same polymer.


https://doi.org/10.1021/acs.macromol.2c02435
Macromolecules 2023, 56, 4267−4277

important, because entanglements between the polymeric probe and the polymer matrix will enhance transfer of the applied force toward the mechanophore.[12] Styrene was polymerized via conventional free-radical polymerization to obtain a short and long matrix polymer: PSS ($M_n \approx 1 \times 10^5$ g·mol$^{-1}$) and PSL ($M_n \approx 6 \times 10^5$ g·mol$^{-1}$). For polycarbonate, no unfunctionalized matrix was added.

**Thermal Stability.** The mechanophores were tested for their thermal stability in both the solid state and solution. The solid-state tests were performed on a hot plate equipped with a thermocouple. A few AM-2Br crystals were put on a piece of aluminum foil on a hotplate and heated to 250 °C. Instantaneous and bright fluorescence was observed around 230 °C, which is close to the melting point of the crystals as measured by differential scanning calorimetry (DSC) ($T_m \approx$ 226 °C, see Figure S4). This suggest that fluorescent anthracene is not released from crystalline AM-2Br until the crystals melt. When AM-2Br was dissolved in *ortho*-dichlorobenzene (*o*-DCB), the anthracene was released at lower temperatures. Percentages of activation were determined using a calibration curve for concentrations between $5 \times 10^{-8}$ M and $5 \times 10^{-6}$ M (Figure S5 and Table S1). The results of these experiments are shown in Figure 1, and it is clear from

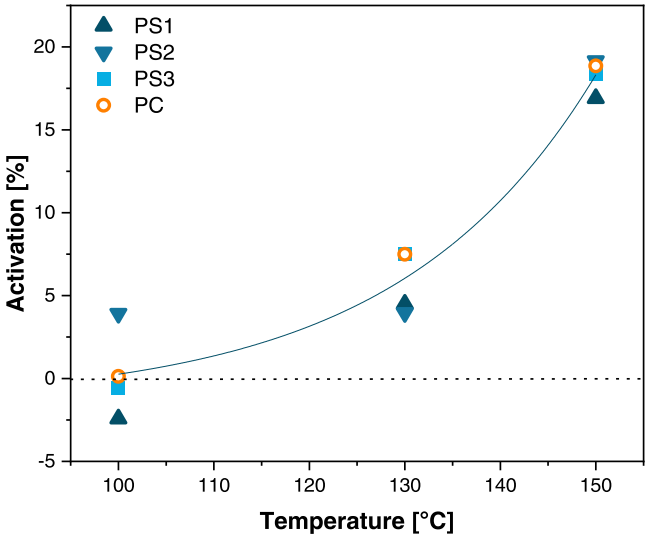


**Figure 1.** Thermal mechanophore activation in *o*-DCB solution after heating PS1 (dark blue triangle), PS2 (light blue inverted triangle), PS3 (blue square), and PC (orange circle) to 100, 130, and 150 °C for 1 h. Activation was calculated from the intensity at 410 nm and was corrected for activation at $t = 0$. The solid line is a guide to the eye, while the dotted line represents 0% activation.

this figure that an increase in temperature leads to an increase in activation. Heating the mechanophore for at least 1 h at 100 °C resulted in only 0.3% of activation; keeping the sample at 100 °C for 24 h, only 3% of the mechanophore was activated. Hence, sample preparation of mechanophore-containing polymer, which takes place below 100 °C, does not result in significant activation of the mechanophore.

**Activation via Sonication.** Ultrasonication was used to investigate the mechanical activation of the DA-adduct in solution. Sonication of a polymer solution with a sonication probe instead of a sonication bath results in cavitation-induced cleavage of polymers. The rate of cleavage is dependent on the molar mass and preferentially takes place in the middle of the polymer chain.[30]

Solutions of $5 \times 10^{-5}$ M of PS1−PS3 and PC were sonicated for a period of 15 min and for a period of 1 h. Fluorescence intensities of the solutions were measured to determine the fractions of activated mechanophores, and the results are shown in Figure 2. The spectra show, as expected, that the

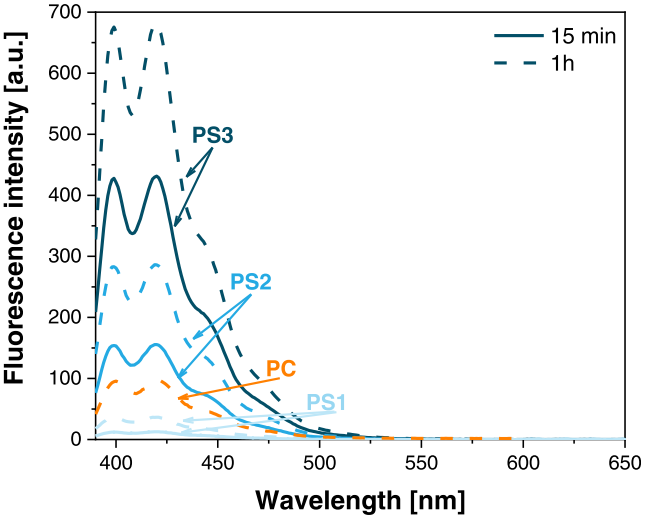


**Figure 2.** Fluorescence emission spectra after sonication of PS1−PS3 for 15 min and 1 h and PC for 1 h. Number-average molar masses for PS1−PS3 and PC are 32, 66, 102, and 31 kg·mol$^{-1}$, respectively.

activation of the mechanophore in solution by sonication increases with the molar mass of the polymer. Percentages of activation were determined from a calibration curve for concentrations between $5 \times 10^{-8}$ and $5 \times 10^{-6}$ M (Table 2, see the SI for details).

**Table 2. Activation of PS1−PS3 and PC after 15 min and 1 h of Sonication**

| | | %activation[aa] | |
|---|---|---|---|
| polymer | $M_n$ [g·mol$^{-1}$] | 15 min sonication | 1 h sonication |
| PS1 | 32 | 0 | 1.4 |
| PS2 | 66 | 3.1 | 12.0 |
| PS3 | 109 | 9.2 | 30.0 |
| PC | 31 | | 2.2 |

[a]Percentages of activation were calculated for each polymer based on fluorescence emission at 411 nm.

PS1 and PC have $M_n \approx 3 \times 10^4$ g·mol$^{-1}$ and both show low mechanophore activation because the molar mass is close to the limiting molar mass for polymers subjected to ultrasonication.[31] For higher molar masses of PS, the activation increased from ~1.5% for PS1 to ~12 and ~30% for PS2 and PS3, respectively. The sonication experiments show that, for all polymers described in this work, the mechanophore can be activated in solution. While the lower molar mass probes have masses close to the limiting molar mass for ultrasonication, the higher molar mass probes show significant activation.

**Solid-State Activation of the Mechanophore.** A variety of techniques were used to study the mechanical activation of the mechanophore in a solid polymer film: grinding, compression, tensile tests, and indentation tests. For


https://doi.org/10.1021/acs.macromol.2c02435
Macromolecules 2023, 56, 4267−4277

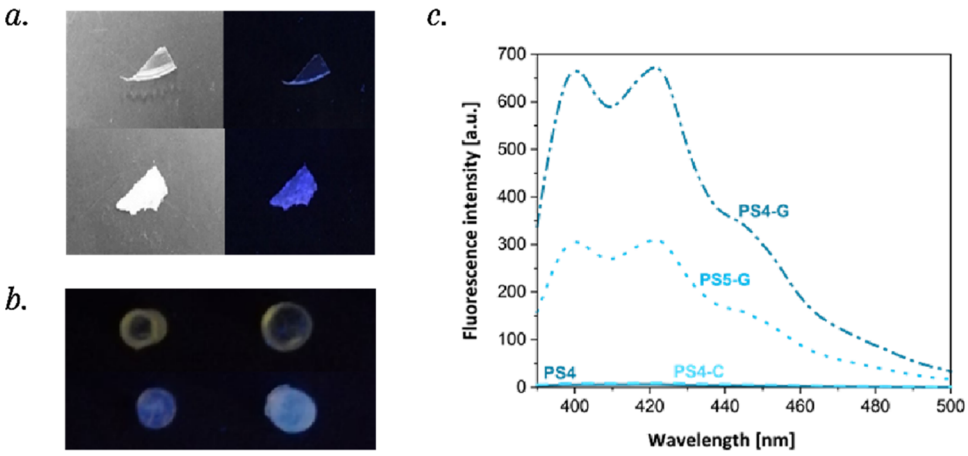


**Figure 3.** (a) PS4 film before (top) and after (bottom) grinding in daylight (left) and with excitation at 366 nm (right). (b) Visualization of the fluorescence obtained before and after compression. Top left: uncompressed commercial polystyrene, top right: compressed commercial polystyrene. Bottom left: uncompressed PS4, and bottom right: compressed PS4. (c) Fluorescence intensity of the dissolved samples (the addition of C behind the sample name indicates a sample after compression; the addition of G indicates a sample after grinding).

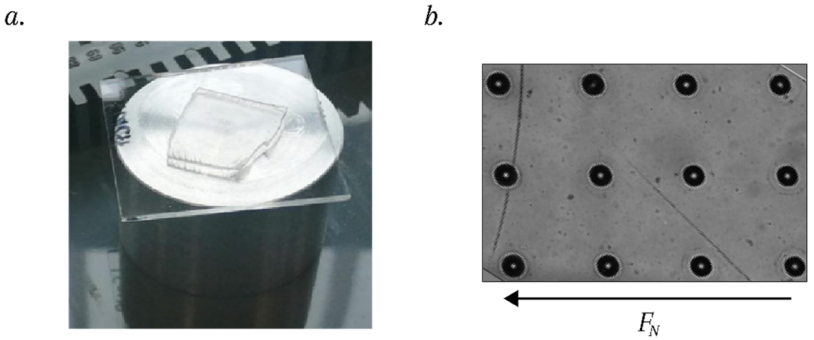


**Figure 4.** (a) Photograph of a sample prepared for indentation and scratch tests. (b) Bright-field image of indentation tests of the five highest forces on PSL-PS1 with different normal loads of 200, 190, 180, and 160 mN from left to right. All indentations were performed in triplicate; each column of indents represent one normal load.

polycarbonate (PC), only tensile and indentation tests were used, whereas the polystyrene samples were tested by grinding, compression, and indentation.

*Compression and Grinding.* Grinding and compression tests were performed on fully mechanophore-functionalized polymers with a number-average molar mass of 51 × $10^3$ g·$mol^{-1}$ (PS4) or 102 × $10^3$ g·$mol^{-1}$ (PS5). Solvent-cast polystyrene films were manually ground for 2 min and subsequently dissolved in toluene. Fluorescence spectroscopy of the dissolved films showed that up to 5% of the mechanophore was activated by grinding (Figure 3a,c). Although direct quantification of activation in the polymeric films was not possible, these experiments clearly showed that the mechanophore can be activated by applying a mechanical force to the polymer film.

Additionally, compression tests were performed on cylinders with a diameter of 3 mm and an aspect ratio of 1 (Figure 3b,c). These cylinders were prepared after solvent casting polystyrene films and stacking in a cylindrical metal mold. After heating the stack of films to 140 °C (which is above $T_g \approx 105$ °C) for 10 min in a Tribotrak and applying a pressure of 14 MPa with a mass of 10 kg on top of the stack of films, the stacked films were permanently attached to each other, and cylindrical polystyrene samples were obtained (see the SI for details). These samples were covered with PTFE tape and compressed with a uniaxial force in a tensile tester. The activation of the mechanophore was determined by dissolving the compressed sample and measuring fluorescence in solution; no change in fluorescence was observed. For polycarbonate, it was impossible to prepare similar samples because the mechanophore is not stable at the required higher temperatures ($T$ needs to be higher than $T_g \approx 140$ °C). Hence, in this case, the mechanophore was activated via tensile tests. These tests were performed at a constant engineering strain rate of 0.001 $s^{-1}$; the region of break was dissolved in THF, and fluorescence was measured. No activation could be detected.

*Indentation Tests.* Indentation and scratch tests were performed on films with a thickness of ∼200 μm for polycarbonate (PC) and between 300 and 400 μm for polystyrene (PS1 mixed with a matrix of PSS or PSL). Thicker PC films were not investigated because they were non-transparent due to solvent-induced crystallization of polycarbonate.[32,33] Transparent films were glued onto a glass plate and aluminum stud to ensure that the samples were flat and immobile during indentation and scratch tests as shown in Figure 4a. Indentation tests were performed at different loads as shown in Figure 4b. At the contact edge between the sample and indenter, stress localization may lead to microcrack formation in radial direction; however, no fluorescence was observed (Figure S8). The penetration depth was slightly lower for PSL-PS1 than for PSS-PS1, but the difference was negligible (see the SI for details).[34]


https://doi.org/10.1021/acs.macromol.2c02435
Macromolecules 2023, 56, 4267−4277

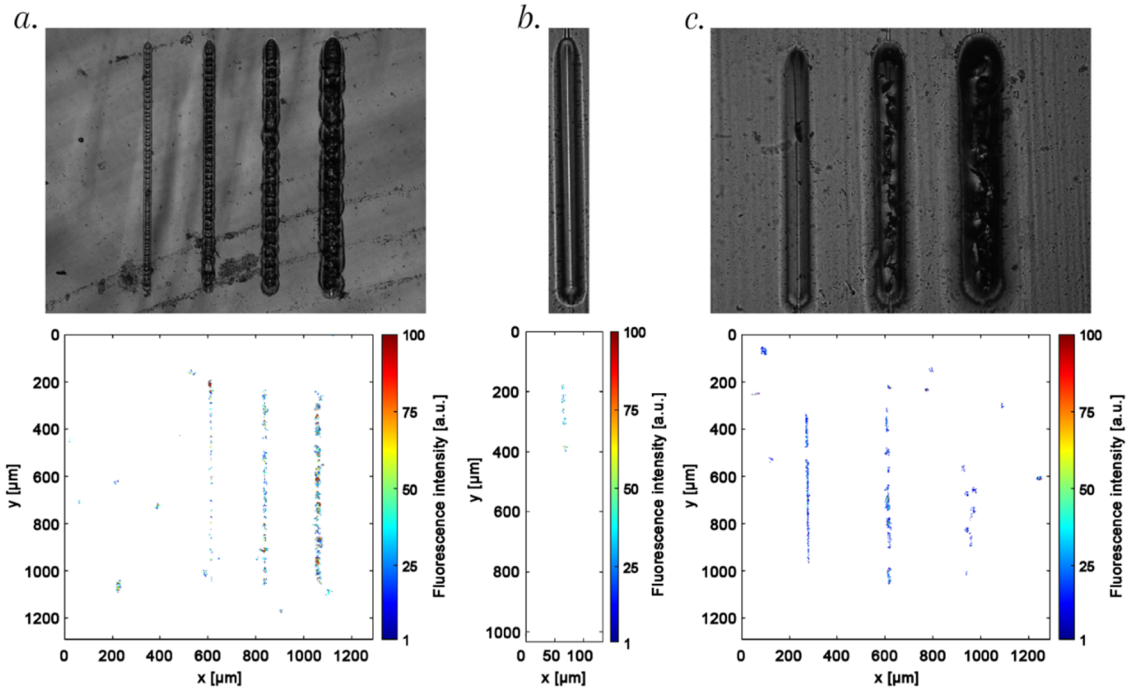


**Figure 5.** Bright-field images (top) and fluorescence intensity plots (bottom) of sliding friction tests (scratch length 0.8 mm) on PSL-PS1 and PC with different normal loads of (a) 50, 100, 200, and 400 mN on polystyrene, (b) 400 mN on PC and (c) 750, 1500, and 3000 mN on PC.

In order to increase the amount of local deformation in a controlled way, single-asperity sliding friction tests, better known as scratch tests, were performed.[35] The friction force generated by the sliding motion increases the local stress state and yields a larger area over which the mechanophore may be activated. These experiments were performed with an indentation machine with a conical tip with a cone angle of 90° and a top radius of 10 $\mu$m. Polymer samples were prepared by casting a mixture of the PS matrix (PSS or PSL) and mechanophore-containing polymer (PS1−PS3) so that the overall amount of mechanophore was 0.2 wt %. The polycarbonate film was cast from a 100% PC solution. These samples were glued onto a glass plate and an aluminum stud (similar to what is shown in Figure 4a) and scratched with a sliding speed of 10 $\mu$m·s$^{-1}$ with applied normal loads ranging between 50 and 400 mN for PS1−PS3 and up to 3000 mN for PC. Bright-field microscopy was used to visualize macroscopic damage to the film, and fluorescence microscopy was used to visualize bond breaking processes in the film. A Matlab (see the SI for details) script was used to transform the fluorescence images into intensity patterns to visualize the activated areas.

In Figure 5, the results are shown for PSL-PS1 and PC (other compositions, see the SI for details). A clear difference in damage is observed between polystyrene and polycarbonate. Scratching polystyrene resulted in clear craze formation at normal loads starting from $F_N$ = 100 mN with corresponding mechanophore activation as shown in the intensity plots in Figure 5. The width of the scratch and the area of mechanophore activation increase with increasing normal force. For polycarbonate, no crack or craze formation and no mechanophore activation were observed below $F_N$ = 400 mN. When a normal force of 400 mN (Figure 5b) was applied to PC, no crazes or cracks were observed and only a minimal amount of activation was observed. An applied normal force of $F_N$ = 750 mN resulted in activation of the mechanophore around the tip without introducing visual cracks in the material. When the normal force was increased to 1500 mN, the polycarbonate started to detach from the glass plate, and thus, the stresses were not concentrated on the sample. This, in turn, resulted in an interrupted fluorescence intensity pattern. An even more strongly interrupted pattern was observed for a scratch test with $F_N$ = 3000 mN as here most of the sample detached from the glass substrate.

In Figure 6a, a comparison between scratches in polystyrene and polycarbonate is shown. PSS, PSS-PS1, and PC were used for sliding friction tests with a normal load of 500 and 1000 mN. PSS is a polystyrene matrix without mechanophore and hence expected to show zero fluorescence, which is indeed what is observed. PC shows a fluorescence intensity around 0 at 500 mN, while for PSS-PS1, a strongly fluctuating fluorescence signal was observed. Doubling the normal force of sliding friction tests to a normal load of $F_N$ = 1000 mN resulted in a steady fluorescence over the total length of the scratch in PC.

This contrast in behavior upon scratching can be explained by the differences in stress distribution in these polymers. Uniaxial compression tests on both polystyrene and polycarbonate show a clear difference in mechanical behavior after the yield point.[26] Polystyrene shows a large strain-softening effect, whereas polycarbonate undergoes some strain softening followed by strong strain hardening, resulting in a delay of local failure.[26] Its resistance to deformation becomes higher at higher loads, which results in a smaller bow wave during the sliding friction tests and a lower lateral friction force.[36] Hence, higher forces are required to reach similar damage in polycarbonate as in polystyrene. When the force is kept the same, higher temperatures accelerate damage in polycarbonate.[26]

The fluorescence intensities show a similar trend as observed for the penetration depth and the friction force plotted against the distance of the scratch (Figures 7a and S10). The friction force in polycarbonate was much lower than the normal force


https://doi.org/10.1021/acs.macromol.2c02435
Macromolecules 2023, 56, 4267−4277

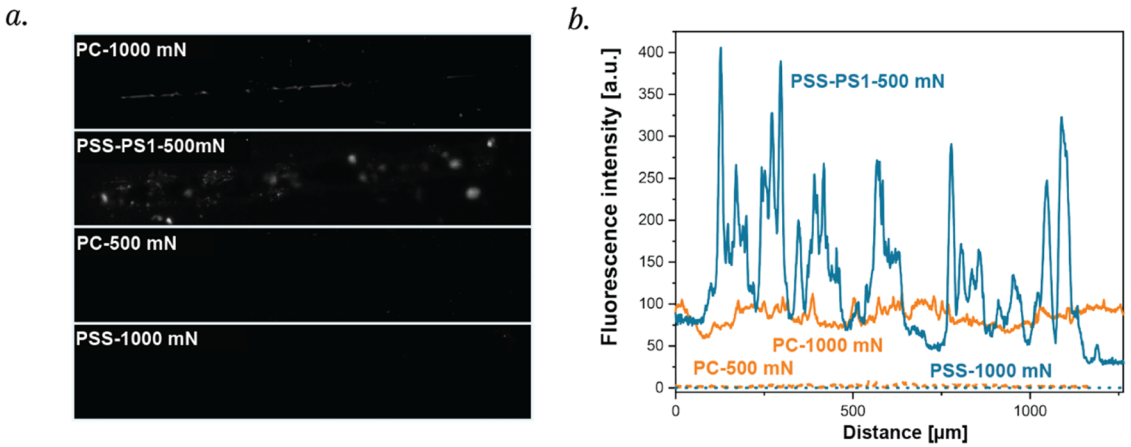


**Figure 6.** Fluorescence microscopy images (left) and intensity plots (right) of PSS, PSS-PS1, and PC scratched with $F_N$ = 500 or 1000 mN. Intensity patterns were taken from the area shown in the microscopy image on the left.

applied to the samples due to its higher strain hardening. In polystyrene, fluctuation around a steady-state value of the applied normal load was observed. When comparing polycarbonate (shown in orange) to polystyrene (shown in blue) in Figure 7, again a clear difference in behavior was observed. Polycarbonate shows a steady friction force and penetration depth up to a normal force of 1500 mN, whereas the friction force and penetration depth in polystyrene start to fluctuate when a normal force of 100 mN or more was applied. The mean value in the steady-state regime of this friction force and penetration depth was plotted vs the load (Figures 7b,c, S11, and S12). It should be noted that the error bars in this case represent an unconventional parameter; rather than being the standard deviation of the mean of three scratches, they here indicate the average of the standard deviation with reference to the mean per individual scratch. This parameter increases sharply at higher loads (between 200 and 300 mN for PS), indicating a larger amplitude of the observed surface instability.

The strongly fluctuating friction force in the polystyrene samples can be explained by the formation of crazes behind the tip, and correlates well with the pattern of mechanophore activation shown in Figure 6. This clearly indicates a direct relation between bond scission and crack formation.

## DISCUSSION AND CONCLUSIONS

In both polycarbonate and polystyrene, bond breaking is localized and hence detection is rather challenging. In solid polymer materials, only sliding friction showed measurable mechanophore activation. Sliding friction tests were performed at different normal forces, and from these tests, a clear difference in the molecular origin of the mechanical behavior between polystyrene and polycarbonate was observed. Polystyrene showed mechanophore activation at normal forces $\geq$ 100 mN and additionally formed crazes in the polymer material. Correlation of the fluorescence intensity pattern with the fluctuating friction force and penetration depth shows that craze formation and bond breaking are closely related in polystyrene. Polycarbonate required higher normal loads for mechanophore activation. It was only activated at a normal force of 400 mN without the formation of visual cracks, suggesting that, in the scratch tests, polycarbonate mainly undergoes plastic deformation with limited rupture of covalent bonds. This is consistent with what is known on the difference in mechanical behavior of both polymers. Polystyrene is known to undergo brittle failure, while polycarbonate is a tougher material.[26] When performing a tensile test, polystyrene breaks at very low strains between 0 and 2%, while for polycarbonate, 70−80% strain can easily be reached.[37,38] This difference can be explained by the post-yield intrinsic behavior of the material.[38] Both polymers show a decrease in stress after the yield point, which is known as strain softening of the polymer, resulting in localization of stress and strain. In polystyrene, this localization is believed to initiate craze formation, while in polycarbonate, the unstable behavior is counteracted by the strain hardening effect, which in the increasing stress at higher strains leads to stable plastic deformation without initiation of macroscopic failure.[26,38] In this study, we have shown that the different mechanical properties of these polymers are associated with pronounced differences in bond breaking behavior.

## EXPERIMENTAL DETAILS

**Materials.** All reagents for the mechanophore synthesis were purchased from Sigma-Aldrich and Merck in >98% purity. NMR solvents from Cambridge Isotopes Laboratories and other solvents from Biosolve were used. All chemicals were used as received unless stated otherwise. Bis(methyl salicyl) carbonate (BMSC, SABIC, 99+%) and bisphenol-A (BPA, SABIC, polymerization grade, >99%) were kindly provided by SABIC. Styrene was purified on an aluminum plug prior to use. Dry solvents were obtained using the MBraun solvent purification system (MB SPS-800). 1,2-Dichlorobenzene was dried over mol sieves (4 Å).

**Instrumentation.** Reactions were monitored by either $^1$H NMR or thin-layer chromatography (TLC). $^1$H NMR and $^{13}$C NMR spectra were recorded at room temperature using a 400 MHz Bruker UltrasSHield Nuclear Magnetic Resonance spectrometer, in $CDCl_3$ or DMSO-$d_6$. DOSY spectra were recorded on the same instrument at room temperature in $CDCl_3$. Acquisition parameters for the proton NMR were set to 124 scans with a relaxation delay of 3 s, and 16 points for the indirect dimensions were measured. Chemical shifts are given in ppm with tetramethyl silane (TMS, 0 ppm) as an internal standard. Column chromatography was performed manually using silica (60−200 $\mu$m, 60 Å) as a stationary phase. Matrix-assisted laser desorption/ionization−time-of-flight mass spectra (MALDI-TOF) were measured using a Bruker Autoflex Speed mass spectrometer using $\alpha$-cyano-4-hydroxycinnamic acid (CHCA) or *trans*-2-[3-(4-*tert*-butylphenyl)-2-methyl-2-propenylidene]-malononitrile (DCBT) as a matrix. Size-exclusion chromatography (SEC) was performed in tetrahydrofuran (THF) at 25 °C on a Shimadzu Prominence-I LC-2030C 3D equipped with an RID-20A detector and calibrated by


https://doi.org/10.1021/acs.macromol.2c02435
Macromolecules 2023, 56, 4267−4277

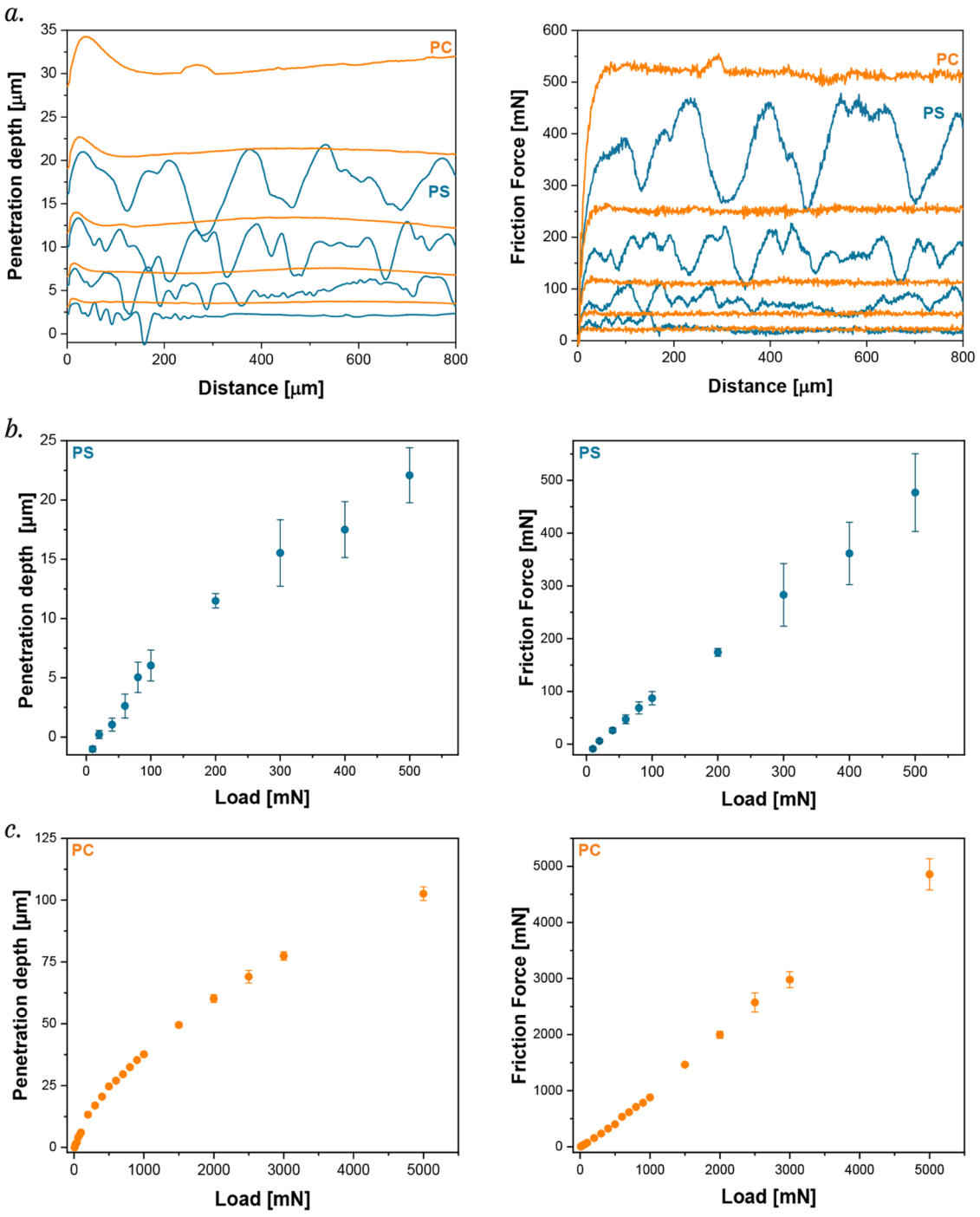


**Figure 7.** Penetration depth (left) and friction force (right) as a function of (a) the distance of the scratch with loads of 50, 100, 200, and 400 mN for polystyrene (blue) and 50, 100, 200, 400, and 750 mN for polycarbonate (orange). A steadier friction force and penetration depth were observed for polycarbonate than for polystyrene. (b) Mean penetration depth and friction force as a function of load for polystyrene. (c) Mean penetration depth and friction force as a function of load for polycarbonate.

narrow polystyrene standards. The following Mark−Houwink−Sakurada parameters were used to convert the polystyrene (PS) masses into polycarbonate (PC) masses: $K_{PS} = 1.41 \times 10^{-4}$ dL·g$^{-1}$, $a_{PS} = 0.70$, $K_{PC} = 4.12 \times 10^{-4}$ dL·g$^{-1}$, $a_{PC} = 0.69$.[39] Fluorescence spectra were recorded on a Jasco FP 6500 fluorescence spectrometer with an excitation wavelength of 366 nm, an excitation and emission slit width of 3 nm, and a scanning speed of 100 nm·min$^{-1}$. Sonication experiments were performed on a QSonica, Q500 sonicator with an amplitude of 30%. For sonication experiments, polymers were dissolved in THF, transferred to a Suslick cell, and cooled to 2 °C. While sonicating without pulse, the solution was bubbled with methane. Differential scanning calorimetry (DSC) measurements were performed on a TA Instruments Q2000 differential scanning calorimeter equipped with an RCS90 cooling accessory using aluminum hermetic pans. For each measurement, 5−10 mg of sample was used. The sample was scanned from 30 to 250 °C at a heating rate of 10 °C·min$^{-1}$, followed by a cooling cycle in the same temperature range at a rate of 10 °C·min$^{-1}$.

*Synthesis of 4,10-Dioxatricyclo[5,2,1,0]dec-8-ene-3,5-dione (**1**).* Maleic anhydride (50 g, 0.51 mol) and furan (55 mL, 0.76 mol) were dissolved in toluene while heating to the desired reaction temperature of 80 °C, and the reaction was left to react overnight. The reaction


https://doi.org/10.1021/acs.macromol.2c02435
Macromolecules 2023, 56, 4267−4277

mixture was left to cool to room temperature, and the precipitate was isolated by filtration. The crystals were washed with diethyl ether and dried under vacuum at 40 °C. The final product was obtained as white crystals in a 78% yield. $^1$H NMR (400 MHz, CDCl3): $\delta$ 6.57 (s, 2H), 5.46 (s, 2H), 3.17 (s, 2H).

*Synthesis of 4-(2-Hydroxy-ethyl)-10-oxa-4-aza-tricyclo-[5.2.1.02,6]dec-8-ene-3,5-dione (**2**).* Compound 1 (55 g, 0.33 mol) and aminoethanol (23 mL, 0.40 mol) were dissolved in methanol (400 mL) refluxed at 67 °C. The mixture was reacted overnight, and solvents were evaporated. The crude product was dissolved in chloroform and extracted with water three times. The organic layer was dried by evaporating chloroform, and the product was obtained as a white solid in a 52% yield. $^1$H NMR (400 MHz, $CDCl_3$): $\delta$ 6.53 (s, 2H) 5.29 (s, 2H) 3.77 (t, 2H) 3.71 (t, $J$ = 4 Hz, 2H) 2.90 (s, 2H). $^{13}$C NMR (400 MHz, $CDCl_3$): $\delta$ 176.81, 136.52, 80.96, 60.11, 47.50, 41.71.

*Synthesis of N-(2-Hydroxyethyl)maleimide (M−OH).* In a 250 mL round bottom flask, compound **2** (8.0 g, 38.3 mmol) was dissolved in 80 mL of toluene. After stirring the mixture for 28 h at 120 °C, the solvent was evaporated in vacuo. M−OH was obtained as off-white crystals in a 98% yield. $^1$H NMR (400 MHz, $CDCl_3$): $\delta$ 6.75 (s, 2H), 3.80 (t, $J$ = 5.2 Hz, 2H), 3.74 (t, $J$ = 5.0 Hz, 2H). $^{13}$C NMR (400 MHz, CDCl3): $\delta$ 171.15, 134.26, 60.93, 40.70.

*Synthesis of 4-(Anthracene-9-yl)phenol (A−OH).* A 1 L three-neck round bottom flask was dried in an oven and equipped with a tap, septum, and cap. 9-Bromoanthracene (4.78 g, 18.3 mmol), 4-hydroxyphenylboronic acid (5.00 g, 36.5 mmol), $K_2CO_3$ (13.15 g, 95.1 mmol), and $Pd(PPh_3)_4$ (1.06 g, 0.9 mmol) were added, and the flask was degassed by three argon purge and refill cycles. 250 mL of dry DMF was added via a canula after which the reaction mixture was heated to 90 °C and reacted for 48 h while stirring under an argon atmosphere. After the reaction, the solid potassium carbonate was removed by filtration and the filtrate was dried in vacuo. The crude product was redissolved in chloroform and extracted twice with demineralized water and once with brine. $Na_2SO_4$ was used to remove water from the chloroform fraction and after filtration. After evaporation of the solvent, the crude product was obtained as a brown solid. The solid was further purified by column chromatography (silica, 4:1 heptane/EtOAc (v/v)), and after drying in vacuo, a yellow solid was obtained in a 78% yield. $^1$H NMR (400 mHz, $CDCl_3$): $\delta$ 8.48 (s, 1H), 8.04 (d, $J$ = 8.5 Hz, 2H), 7.71 (dd, $J$ = 8.8, 1.0 Hz, 2H), 7.51−7.39 (m, 2H), 7.39−7.27 (m, 4H), 7.12−6.99 (m, 2H), 5.01 (s, 1H). $^{13}$C NMR (400 MHz, $CDCl_3$): $\delta$ 155.00, 136.69, 132.52, 131.42, 131.04, 130.54, 128.35, 126.87, 126.43, 125.27, 125.08, 115.31.

*Synthesis of Diels−Alder Diol (AM-2OH).* A−OH (4.2 g, 15.6 mmol) and M−OH (2.2 g, 15.6 mmol) were added to an oven-dried 1 L round bottom flask. The reactants were dissolved in a mix of 250 mL of toluene and 125 mL of isopropanol. The reaction mixture was heated to 100 °C and reacted overnight. Low conversions were observed, and the reaction temperature was increased to 110 °C. The mixture was stirred for 48 h and dried in vacuo. An off-white solid was obtained and further purified by stirring the solid in chloroform and filtering on a glass filter. This step was repeated three times. After filtration, the residue was dried in a vacuum oven at 40 °C. AM-2OH was obtained as a white solid powder in an 83% yield. $^1$H NMR (400 MHz, DMSO-$d_6$): $\delta$ 9.58 (s, 1H), 7.83 (s, 1H), 7.51 (d, $J$ = 6.9 Hz, 1H), 7.31 (d, $J$ = 6.9 Hz, 1H), 7.24−6.86 (m, 8H), 6.31 (d, $J$ = 7.6 Hz, 1H), 4.84 (d, $J$ = 3.0 Hz, 1H), 4.58 (t, $J$ = 5.8 Hz, 1H), 4.00 (d, $J$ = 8.3 Hz, 1H), 3.28 (dd, $J$ = 8.2, 3.0 Hz, 1H), 2.94 (t, $J$ = 6.8 Hz, 2H), 2.54 (t, $J$ = 8.0 Hz, 2H). $^{13}$C NMR (400 MHz, DMSO-$d_6$): $\delta$ 176.38, 175.56, 156.82, 146.10, 141.57, 141.18, 139.40, 133.37, 131.77, 126.94, 126.90, 126.55, 126.37, 125.99, 125.42, 125.22, 124.93, 123.90, 114.93, 56.83, 55.39, 48.93, 46.91, 45.59. Maldi-TOF MS: $m/z$ calculated $(M + Na)^+$: 434.14; found 434.09.

*Synthesis of N-[2-(2-Bromoisobutyryloxy)ethyl]maleimide(M−Br).* A three-neck round bottom flask was equipped with a bubbler, a septum, and a cap. M−OH (2.50 g, 17.7 mmol) was dissolved in 100 mL of dry dichloromethane (DCM), and triethylamine (2.84 mL, 20.41 mmol) was added under argon flow. The mixture was put on ice for 20 min, and a solution of $\alpha$-bromoisobutyryl bromide (2.52 mL, 20.41 mmol) in 30 mL of dry DCM was added dropwise to the reaction mixture. The reaction was left for 3 h and allowed to warm to room temperature. After the reaction, the mixture was filtered and DCM was evaporated; the obtained solid was redissolved in chloroform and washed with 5% $NaHCO_3$, demineralized water, and brine subsequently. The chloroform fraction was dried in vacuo. The crude product was further purified by column chromatography over silica using 100% chloroform. M-Br was obtained as a white solid in a 64% yield. $^1$H NMR (400 MHz, $CDCl_3$): $\delta$ 6.73 (s, 2H), 4.33 (t, $J$ = 5.6 Hz, 2H), 3.86 (t, $J$ = 5.3 Hz, 2H), 1.89 (s, 6H). $^{13}$C NMR (400 MHz, $CDCl_3$): $\delta$ 171.62, 170.33, 134.27, 62.89, 55.45, 36.60, 30.61. Maldi-TOF MS: $m/z$ calculated $(M + Na)^+$: 311.98; found 311.94

*Synthesis of 4-(Anthracen-9-yl)phenyl 2-Bromo-2-methylpropanoate (A−Br).* A three-neck round bottom flask was equipped with a bubbler, a septum, and a cap. A−OH (2.05 g, 7.3 mmol) was dissolved in 100 mL dry DCM, and triethylamine (2.05 mL, 14.8 mmol) was added under argon flow. The mixture was put on ice for 20 min, and a solution of $\alpha$-bromoisobutyryl bromide (1 mL, 8.8 mmol) in 30 mL of dry DCM was added dropwise to the reaction mixture. The reaction was left for 3 h and allowed to warm to room temperature. The crude product was further purified by flushing over a silica plug in 100% chloroform and recrystallization in MeOH. A−Br was filtered off and dried in vacuo resulting in 2.1 g off-white powder (67%). $^1$H NMR (400 MHz, DMSO-$d_6$): $\delta$ 8.49 (s, 1H), 8.05 (d, $J$ = 8.51 2H), 7.65 (d, $J$ = 8.51, 2H), 7.47 (m, 4H), 7.37 (m, 4H), 2.16 (s, 6H).

*Synthesis of the Diels−Alder ATRP Initiator (AM-2Br).* *N*-[2-(2-Bromoisobutyryloxy)ethyl]maleimide (1.714 g, 5.9 mmol) and 4-(anthracen-9-yl)phenyl 2-bromo-2-methylpropanoate (2.481 g, 5.9 mmol) were added to an oven-dried 250 mL round bottom flask. The reactants were dissolved in 82 mL of 2:1 toluene/isopropyl alcohol (v/v). The reaction mixture was heated to 120 °C and reacted for 2 days under reflux while stirred. After the reaction, the solvent was evaporated via a rotary evaporator. The obtained crude product was further purified via column chromatography (silica, 2:1 hexane/EtOAc (v/v)). Two fractions were obtained, and the second fraction containing the product was further purified via column chromatography (silica, 2:1 hexane/EtOAc (v/v)). After evaporation of the solvent and drying in the vacuum oven AM-2Br was obtained in the form of white needles in a yield of 80%. $^1$H NMR (400 MHz, $CDCl_3$): $\delta$ 8.11 (s, 1H), 7.51−7.29 (m, 5H), 7.25−7.13 (m, 4H), 7.03 (td, $J$ = 7.6, 1.3 Hz, 1H), 6.48 (d, $J$ = 7.7 Hz, 1H), 4.87 (d, $J$ = 3.0 Hz, 1H), 3.90 (d, $J$ = 8.4 Hz, 1H), 3.70−3.51 (m, 2H), 3.44−3.20 (m, 3H), 2.14 (s, 6H), 1.88 (s, 3H), 1.86 (s, 3H). $^{13}$C NMR (400 MHz, $CDCl_3$): $\delta$ 175.79, 174.88, 170.26, 150.12, 140.12, 138.31, 127.26, 127.12, 126.89, 126.52, 125.51, 125.24, 125.10, 123.42, 61.97, 55.98, 55.62, 55.44, 49.12, 47.19, 46.13, 36.68, 30.70. Maldi-TOF MS: $m/z$ calculated $(M + Na)^+$: 732.04; found 731.99.

*Synthesis of PSS and PSL—Conventional Free-Radical Polymerization.* A flame-dried Schlenk flask was charged with styrene, toluene, and AIBN and kept on ice to avoid initiation of the polymerization. The reaction mixture was bubbled with argon for 20 min and afterward heated to 75 °C. The reaction was left stirring under an inert atmosphere overnight. The viscous reaction mixture was precipitated as a polymer into MeOH, and the polymer was isolated via filtration and dried at 40 °C under vacuum. Details for the polymerizations are shown in Table 3.

**Table 3. Reaction Conditions for the Free-Radical Polymerization of Polystyrene**

| polymer | styrene (mL) | toluene (mL) | AIBN (mg) | $m^a$ (g)$^a$ | $M_n^{bb}$ ($10^3$ g·mol$^{-1}$) | $Đ^{cc}$ |
|---|---|---|---|---|---|---|
| PSS | 33 | 67 | 32 | 9.9 | 107 | 1.8 |
| PSL | 48 | 12 | 1 | 16.4 | 560 | 1.9 |

[a]Obtained mass of the polymer. [b]Number-average molar mass as determined by SEC. [c]$Đ \equiv M_w/M_n$ as determined by SEC.



https://doi.org/10.1021/acs.macromol.2c02435
Macromolecules 2023, 56, 4267−4277

Table 4. Reaction Conditions for the SET-LRP PS1−PS5

| polymer | initiator [$10^{-4}$ mol] | styrene [mL] | toluene [mL] | reaction time [h] | $m^{aa}$ [g] | $M_n{}^{bb}$ [$10^3$ g·mol$^{-1}$] | $Đ^{cc}$ |
|---|---|---|---|---|---|---|---|
| PS1 | 1.4 | 22.5 | 20 | 69 | 2.4 | 32 | 1.2 |
| PS2 | 1.4 | 48 | 0 | 76 | 10.8 | 66 | 1.5 |
| PS3 | 1.4 | 48 | 0 | 96 | 12.9 | 109 | 1.2 |
| PS4 | 0.7 | 12.2 | 11.5 | 140 | | 51 | 1.4 |
| PS5 | 0.7 | 24 | 0 | 72 | 5.3 | 102 | 1.3 |

[a]Obtained mass of the polymer after precipitation. [b]Number-average molar mass as determined by SEC. [c]$Đ \equiv M_w/M_n$ as determined by SEC.

**Synthesis of PS1−PS3—SET-LRP.** A flame-dried Schlenk flask was charged with AM-2Br (0.10 g, 0.14 mmol), copper(II)bromide (1.62 mg, 0.007 mmol), styrene, and toluene (for used quantities, see Table 4). The reaction mixture was put on ice and bubbled with argon for 20 min. A 5 cm copper wire ($Cu^0$) was wound around a tweezer tip and activated by immersing it in pure HCl for 30 s and rinsing twice with demineralized water, followed by acetone. 10 μL of *N*,*N*,*N*′,*N*″,*N*″-pentamethyldiethylenetriamine (0.04 mmol) was added to the reaction mixture. The reaction was followed by SEC and stopped when the desired molar mass was reached or the dispersity started to increase. The viscous reaction mixture was filtered over basic alumina to remove the copper, and afterward, the polymer was precipitated in MeOH. The resulting precipitate was isolated by filtration and dried at 40°C under vacuum overnight, yielding a white solid.

**Synthesis of PC—Solution Trans Carbonation.** A flame-dried Schlenk flask was charged with BPA (5.1 g, 22.3 mmol), BMSC (6 g, 22.5 mmol), and NaOH (2 mg). This solid mixture was flushed with argon, and 48 mL of *ortho*-dichlorobenzene (*o*-DCB) was added. The resulting reaction mixture was heated to 60 °C while stirring under argon. After 28 h, the reaction was left to cool to room temperature overnight. A viscous white gel-like mixture was obtained. Chloroform was added to dilute to a transparent viscous mixture, and afterward, the polymer was precipitated into a 15-fold excess of *n*-hexane. The resulting white polymer was collected by filtration and dried in a vacuum oven at 40 °C overnight. Afterward, the polymer (3 g) was redissolved in *o*-DCB at 120 °C and AM-2OH (33 mg, 0.08 mmol) was added. The reaction mixture was stirred overnight at 120 °C under inert atmosphere. Then, the mixture was left to cool to room temperature overnight and precipitated in a 15-fold excess of *n*-hexane to obtain PC as a white solid.

**Sample Preparation—Solvent Casting Polystyrene.** 1.25 g of PS was dissolved in 5 mL of toluene and cast into an aluminum mold with a diameter of 4 cm. The films were slowly dried under a nitrogen flow in an oven to avoid bubble formation. The film was left at room temperature overnight and another night at 35 °C. Then, the temperature was increased by 5 °C·h$^{-1}$ and the sample was left overnight at 65 °C. Afterward, the temperature was again increased stepwise to 105 °C and left overnight. The next day, the samples were moved to a vacuum oven for the last drying at 105 °C under vacuum for 12 h.

**Sample Preparation—Solvent Casting Polycarbonate.** 1.35 g of PC was dissolved in 9 mL of DCM and cast into an aluminum mold with a diameter of 7.5 mm. The film was dried in a nitrogen oven overnight at room temperature. Afterward, the temperature was increased to 45 °C and the film was left overnight. Afterward, the film was put into a vacuum oven at 105 °C for 12 h.

**Thermal Stability Testing.** The thermal stability for the polymeric mechanophores was determined in 6 × $10^{-4}$ M in *o*-DCB. Samples were heated to 100, 130, and 150 °C, and the solvent was evaporated and redissolved in THF (1.5 × $10^{-4}$ M). Samples were diluted 100 times before recording the spectra.

**Mechanical Testing—Tensile and Compression Tests.** Dog bone samples with a gauge length of 15 mm and a width of 5 mm were stamped from solvent-cast polycarbonate films. For compression, samples were prepared as a cylinder with an aspect ratio of 1 (see the SI for details). Both tensile and compression tests were performed at a strain rate of 0.001 s$^{-1}$.

**Mechanical Testing—Sliding Friction Experiment Tests.** Single-asperity sliding friction experiments were performed on a CSM Micro Indentation Tester. A defined normal load and sliding velocity were applied to the sample, and the surface penetration and lateral force were measured. A conical, diamond indenter tip geometry, with a cone angle of 90° and a top radius of 10 μm was used to apply normal loads ranging from 50 to 4000 mN. Two rotational motors control the linear, in-plane motion and are able to apply sliding velocities over three decades of magnitude. Scratch tests with lengths of 0.8 and 1 mm were performed at scratch velocities 10 μm·s$^{-1}$, all at room temperature. Each combination of sliding velocity and normal force was applied at least three times to check reproducibility of the steady-state penetration depth and friction force.

**Mechanical Testing—Indentation Tests.** Indentation tests were performed on a MTS Nano Indentor XP equipped with a cylindrical 10 μm flat punch. Load-controlled experiments were performed at a loading rate of 1 mN·s$^{-1}$. Maximum loads were varied between 10 and 200 mN, and all indents were performed in threefold.

**Fluorescence Microscopy.** The glass plates were removed from the aluminum studs, and the back side was cleaned with acetone and dried with dry nitrogen gas. Images were recorded on a Leica SP8 inverted confocal microscope. The microscope was equipped with a camera for bright-field and wide-field fluorescent imaging, and images were recorded in unidirectional scan mode with a pinhole of 1 Airy (151 μm). Mechanophore activation was visualized by using a 405 nm laser excitation combined with a hybrid detector.

## ■ ASSOCIATED CONTENT

### Supporting Information

The Supporting Information is available free of charge at https://pubs.acs.org/doi/10.1021/acs.macromol.2c02435.

Synthetic details and characterization results of the mechanophore-containing polymers; fluorescence calibration curve; details on sample preparation; and mechanophore activation and scratch tests (PDF)

## ■ AUTHOR INFORMATION


### Corresponding Authors

**Rint P. Sijbesma** − *Institute for Complex Molecular Systems, Laboratory of Supramolecular Polymer Chemistry, Department of Chemical Engineering and Chemistry, Eindhoven University of Technology, 5600 MB Eindhoven, The Netherlands;* orcid.org/0000-0002-8975-636X; Email: r.p.sijbesma@tue.nl

**Johan P.A. Heuts** − *Institute for Complex Molecular Systems, Laboratory of Supramolecular Polymer Chemistry, Department of Chemical Engineering and Chemistry, Eindhoven University of Technology, 5600 MB Eindhoven, The Netherlands;* orcid.org/0000-0002-9505-8242; Email: j.p.a.heuts@tue.nl

### Authors

**Annelore Aerts** − *Dutch Polymer Institute, 5600 AX Eindhoven, The Netherlands; Institute for Complex*




https://doi.org/10.1021/acs.macromol.2c02435
Macromolecules 2023, 56, 4267−4277

*Molecular Systems, Laboratory of Supramolecular Polymer Chemistry, Department of Chemical Engineering and Chemistry, Eindhoven University of Technology, 5600 MB Eindhoven, The Netherlands*

**Stan F.S.P. Looijmans** − *Dutch Polymer Institute, 5600 AX Eindhoven, The Netherlands; Polymer Technology, Department of Mechanical Engineering, Eindhoven University of Technology, 5600 MB Eindhoven, The Netherlands;* orcid.org/0000-0002-4148-8351

**Lambèrt C.A. van Breemen** − *Polymer Technology, Department of Mechanical Engineering, Eindhoven University of Technology, 5600 MB Eindhoven, The Netherlands;* orcid.org/0000-0002-0610-1908

Complete contact information is available at: https://pubs.acs.org/10.1021/acs.macromol.2c02435

### Funding

This work was funded by the Dutch Polymer Institute (#805t15).

### Notes

The authors declare no competing financial interest.

Part of this work has been published in the PhD Thesis of Dr Aerts: https://research.tue.nl/files/197469091/20220322_Aerts_hf.pdf

## ■ ACKNOWLEDGMENTS

The authors gratefully acknowledge Dr Jessica Clough for providing part of the Matlab script used for the intensity plots. The Dutch Polymer Institute is gratefully acknowledged for funding; this work forms part of the research program of DPI, project #805t15.

## ■ REFERENCES

(1) Dry, C. Procedures Developed for Self-Repair of Polymer Matrix Composite Materials. *Compos. Struct.* **1996**, *35*, 263−269.

(2) Dry, C.; McMillan, W. A Novel Method to Detect Crack Location and Volume in Opaque and Semi-Opaque Brittle Materials. *Smart Mater. Struct.* **1997**, *6*, 35−39.

(3) Awaja, F.; Zhang, S.; Tripathi, M.; Nikiforov, A.; Pugno, N. Cracks, Microcracks and Fracture in Polymer Structures: Formation, Detection, Autonomic Repair. *Prog. Mater. Sci.* **2016**, *83*, 536−573.

(4) Azadi, M.; Saeedi, M.; Mokhtarishirazabad, M.; Lopez-Crespo, P. Effects of Loading Rate on Crack Growth Behavior in Carbon Fiber Reinforced Polymer Composites Using Digital Image Correlation Technique. *Composites, Part B* **2019**, *175*, No. 107161.

(5) Pang, J. W. C.; Bond, I. P. A Hollow Fibre Reinforced Polymer Composite Encompassing Self-Healing and Enhanced Damage Visibility. *Compos. Sci. Technol.* **2005**, *65*, 1791−1799.

(6) Clarijs, C. C. W. J.; Kanters, M. J. W.; van Erp, M. J.; Engels, T. A. P.; Govaert, L. E. Predicting Plasticity-Controlled Failure of Glassy Polymers: Influence of Stress-Accelerated Progressive Physical Aging. *J. Polym. Sci., Part B: Polym. Phys.* **2019**, *57*, 1300−1314.

(7) Meijer, H. E. H.; Govaert, L. E. Mechanical Performance of Polymer Systems: The Relation between Structure and Properties. *Prog. Polym. Sci.* **2005**, *30*, 915−938.

(8) Yuan, Y.; Chen, Y.- l. Visualized Bond Scission in Mechanically Activated Polymers. *Chin. J. Polym. Sci.* **2017**, *35*, 1315−1327.

(9) Caruso, M. M.; Davis, D. A.; Shen, Q.; Odom, S. A.; Sottos, N. R.; White, S. R.; Moore, J. S. Mechanically-Induced Chemical Changes in Polymeric Materials. *Chem. Rev.* **2009**, *109*, 5755−5798.

(10) Li, M.; Zhang, Q.; Zhou, Y. N.; Zhu, S. Let Spiropyran Help Polymers Feel Force! *Prog. Polym. Sci.* **2018**, *79*, 26−39.

(11) Boulatov, R. *Polymer Mechanochemistry*; Springer: Switzerland, 2015; Vol. *53*.

(12) Chen, Y.; Mellot, G.; Van Luijk, D.; Creton, C.; Sijbesma, R. P. Mechanochemical Tools for Polymer Materials. *Chem. Soc. Rev.* **2021**, *50*, 4100−4140.

(13) Ducrot, E.; Chen, Y.; Bulters, M.; Sijbesma, R. P.; Creton, C. Toughening Elastomers with Sacrificial Bonds and Watching Them Break. *Science* **2014**, *344*, 186−189.

(14) Davis, D. A.; Hamilton, A.; Yang, J.; Cremar, L. D.; Van Gough, D.; Potisek, S. L.; Ong, M. T.; Braun, P. V.; Martínez, T. J.; White, S. R.; Moore, J. S.; Sottos, N. R. Force-Induced Activation of Covalent Bonds in Mechanoresponsive Polymeric Materials. *Nature* **2009**, *459*, 68−72.

(15) Chen, Y.; Spiering, A. J. H.; Karthikeyan, S.; Peters, G. W. M.; Meijer, E. W.; Sijbesma, R. P. Mechanically Induced Chemiluminescence from Polymers Incorporating a 1,2-Dioxetane Unit in the Main Chain. *Nat. Chem.* **2012**, *4*, 559−562.

(16) Yoshie, N.; Saito, S.; Oya, N. A Thermally-Stable Self-Mending Polymer Networked by Diels-Alder Cycloaddition. *Polymer* **2011**, *52*, 6074−6079.

(17) Aerts, A.; Lugger, S. J. D.; Heuts, J. P. A.; Sijbesma, R. P. Pyranine Based Ion-Paired Complex as a Mechanophore in Polyurethanes. *Macromol. Rapid Commun.* **2021**, *42*, No. 2000476.

(18) Lakowicz, J. R. *Principles of Fluorescence Spectroscopy*, 3rd ed.; Springer: Baltimore, 2006.

(19) Göstl, R.; Sijbesma, R. P. Π-Extended Anthracenes As Sensitive Probes for Mechanical Stress. *Chem. Sci.* **2016**, *7*, 370−375.

(20) Beiermann, B. A.; Kramer, S. L. B.; Moore, J. S.; White, S. R.; Sottos, N. R. Role of Mechanophore Orientation in Mechanochemical Reactions. *ACS Macro Lett.* **2012**, *1*, 163−166.

(21) Beiermann, B. A.; Davis, D. A.; Kramer, S. L. B.; Moore, J. S.; Sottos, N. R.; White, S. R. Environmental Effects on Mechanochemical Activation of Spiropyran in Linear PMMA. *J. Mater. Chem.* **2011**, *21*, 8443−8447.

(22) Kim, J. W.; Jung, Y.; Coates, G. W.; Silberstein, M. N. Mechanoactivation of Spiropyran Covalently Linked Pmma: Effect of Temperature, Strain Rate, and Deformation Mode. *Macromolecules* **2015**, *48*, 1335−1342.

(23) Yamamoto, T.; Aoki, D.; Otsuka, H. Polystyrene Functionalized with Diarylacetonitrile for the Visualization of Mechanoradicals and Improved Thermal Stability. *ACS Macro Lett.* **2021**, *10*, 744−748.

(24) Vidavsky, Y.; Yang, S. J.; Abel, B. A.; Agami, I.; Diesendruck, C. E.; Coates, G. W.; Silberstein, M. N. Enabling Room-Temperature Mechanochromic Activation in a Glassy Polymer: Synthesis and Characterization of Spiropyran Polycarbonate. *J. Am. Chem. Soc.* **2019**, *141*, 10060−10067.

(25) Davis, C. S.; Rencheck, M. L.; Woodcock, J. W.; Beams, R.; Wang, M.; Stranick, S.; Forster, A. M.; Gilman, J. W. Activation of Mechanophores in a Thermoset Matrix by Instrumented Scratch. *ACS Appl. Mater. Interfaces* **2021**, *13*, 55498−55506.

(26) Looijmans, S. F. S. P.; de Bie, V. G.; Anderson, P. D.; van Breemen, L. C. A. Hydrostatic Stress as Indicator for Wear Initiation in Polymer Tribology. *Wear* **2019**, *426*−*427*, 1026−1032.

(27) Kamps, J. H.; Groote, R.; Baus, M.; Vermeulen, H.; Hoeks, T.; van der Heijden, R.; Sijbesma, R. P.; Heuts, J. P. A. Activated Carbonates: Enabling the Synthesis of Differentiated Polymers via Solution Carbonation. *Eur. Polym. J.* **2020**, *135*, No. 109901.

(28) Aerts, A.; Kroonen, C.; Kamps, J. H.; Sijbesma, R. P.; Heuts, J. P. A. High Molar Mass Polycarbonate via Dynamic Solution Transcarbonation Using Bis(Methyl Salicyl) Carbonate, an Activated Carbonate. *Macromol. Chem. Phys.* **2021**, *222*, No. 2100186.

(29) Wool, R. P. Polymer Entanglements. *Macromolecules* **1993**, *26*, 1564−1569.

(30) Odell, J. A.; Muller, A. J.; Narh, K. A.; Keller, A. Degradation of Polymer Solutions in Extensional Flows. *Macromolecules* **1990**, *23*, 3092−3103.

(31) May, P. A.; Moore, J. S. Polymer Mechanochemistry: Techniques to Generate Molecular Force via Elongational Flows. *Chem. Soc. Rev.* **2013**, *42*, 7497−7506.

(32) Ruvolo-filho, A.; Murakami, M. M. Transport Properties of Water in Glassy Polycarbonate Films. Effects of the Processing and Thickness. *J. Macromol. Sci., Part B* **1998**, *37*, 627−643.
(33) Su, Y.; Ran, S.; Fang, Z.; Guo, Z. Fullerene-Induced Crystallization toward Improved Mechanical Properties of Solvent Casting Polycarbonate Films. *Appl. Phys. A* **2020**, *126*, No. 293.
(34) Erukhimovich, I.; de la Cruz, M. O.Phase Equilibria and Charge Fractionation in Polydisperse Polyelectrolyte Solutions. 2004, arXiv:cond-mat/0406218. arXiv.org e-Printarchive. https://arxiv.org/abs/cond-mat/0406218.
(35) Briscoe, B. J.; Pelillo, E.; Sinha, S. K. Scratch Hardness and Deformation Maps for Polycarbonate and Polyethylene. *Polym. Eng. Sci.* **1996**, *36*, 2996−3005.
(36) Van Breemen, L. C. A.; Govaert, L. E.; Meijer, H. E. H. Scratching Polycarbonate: A Quantitative Model. *Wear* **2012**, *274*−*275*, 238−247.
(37) Milisavljević, J.; Petrović, E.; Ćirić, I.; Mančić, M.; Marković, D.; Dordević, M. In *Tensile Testing for Different Types of Polymers*; 29th Danubia−Adria Symposium on Advances in Experimental Mechanics DAS 2012, 2012; pp 266−269.
(38) Smit, R. J. M.; Brekelmans, W. A. M.; Meijer, H. E. H. Predictive Modelling of the Properties and Toughness of Polymeric Materials: Part I Why Is Polystyrene Brittle and Polycarbonate Tough? *J. Mater. Sci.* **2000**, *35*, 2855−2867.
(39) Mori, S.; Barth, H. G. *Size Exclusion Chromatography*; Springer-Verlag, 1999.





https://doi.org/10.1021/acs.macromol.2c02435
*Macromolecules* 2023, 56, 4267−4277